BEAM DYNAMICS STUDIES FOR THE SCREX-ISOLDE LINAC AT CERN

M. Pasini*, D. Voulot, CERN, Geneva, Switzerland
M. A. Fraser, R. M. Jones, Cockcroft Institute, UK and University of Manchester, Manchester, UK

Abstract

For the REX-ISOLDE upgrade a superconducting linac based on 101.28 MHz Quarter Wave Resonators (QWRs) is foreseen downstream of the normal conducting (NC) linac. Currently the REX-ISOLDE linac can accelerate ions with a mass to charge ratio in the range of $3 < \mathrm{A/q} < 4.5$ up to an energy of 2.8 MeV/u. The upgrade aims to reach a minimum final beam energy of 10 MeV/u for A/q=4.5 in two main stages. The first stage consists of installing two cryomodules loaded with 10 cavities able to reach 5.5 MeV/u at the end of the present linac and the second consists of replacing part of the existing NC linac and adding further cryomodules. We report here on a beam dynamics study of the accelerator for the two installation stages.

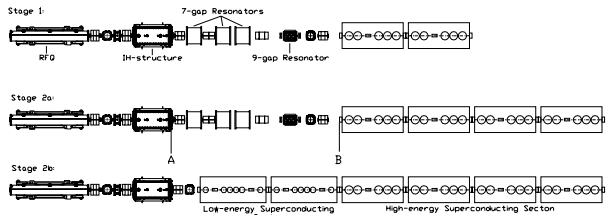

Figure 1: A Schematic of the HIE-ISOLDE linac stages. Stage 1 is shown at the top, while stage 2 can be split into two sub-stages depending on the physics priorities: the low energy cryomodules will allow the delivery of a beam with better emittance; the high energy cryomodule will enable the maximum energy to be reached.

INTRODUCTION

The REX-ISOLDE linac for the ISOLDE Radioactive Ion Beam facility at CERN [1] consists of a normal conducting linac where the RIB gets accelerated in different stages: a 101.28 MHz 4-rod Radio Frequency Quadrupole (RFQ) takes the beam from 5 to 300 keV/u, a 101.28 MHz interdigital drift tube (IH) structure boosts the beam energy up to 1.2 MeV/u, three 101.28 MHz split ring cavities accelerate to reach 2.2 MeV/u and a final 202.56 MHz IH structure is used to vary the energy between 2.2 and 3 MeV/u. The HIE-ISOLDE project [2] looks at the overall upgrade of the facility, i.e. an increase of the final energy of the radioactive ion beam, an improvement of the beam quality and flexibility and an increase of the beam intensity. The linac upgrade will consist of a superconducting machine [3] providing 39.6 MV of effective accelerating voltage with an average synchronous phase ϕ_s of -20 deg. utilising 32 101.28 MHz QWRs split into two families: *low* and *high* β cavities. The first stage of the upgrade plan consists of installing 10 high β cavities grouped in two cryomodules downstream of the present NC linac (stage 1). The second stage will be installed in two parts. Firstly, two more high β cryomodules will be added (stage 2a) downstream from those in stage 1 and secondly the split ring cavities and the 202.56 MHz IH cavity will be replaced with 12 low β cavities grouped in 2 cryomodules (stage 2b). Figure 1 shows a schematic of the different installation stages. The final energy for stage 1 and stage 2 is respectively 5.5 MeV/u and 10 MeV/u for A/q=4.5.

The focusing scheme foresees the employment of 200 mm long SC solenoids, which allow a high mismatch factor tolerance with respect to a standard triplet or doublet focusing scheme [4]. This brings a significant advantage for the tuning and operation of the machine. In fact, RIBs accelerators in general make use of a *high* intensity stable beam as a pilot beam with an A/q ratio that is as close as possible to the A/q of the wanted RIB. This is in fact necessary, since the very low RIB's intensity is practically invisible to conventional beam instrumentation. Once the pilot beam is established, a scaling action is performed and a focusing lattice with high mismatch tolerance guarantees better beam transport in the machine after scaling, where possible beam mismatch can occur. In addition, because SC solenoids allow the intermodule distance to be minimized, the longitudinal acceptance of the linac is not reduced and multi-charge state acceleration can be performed [5]. A schematic of the two cryomodules is shown in Figure 2. With this configuration the beam diagnostics instruments are ideally positioned at the beam waist location in the inter-cryomodule region where a pair of steering magnets will also be installed.

BEAM DYNAMICS SIMULATIONS

For the simulations of the complete HIE-LINAC (stage 2b) a 1 m long matching section with 4 quadrupoles between the first IH-structure and the first cryomodule is taken into account. It is important to keep this section as short as possible in order to minimize the longitudinal beam debunching. The input beam parameters for the simulations are constrained by the IH-cavity output beam and were calculated using `TRACE3D` [6]. The resonators were set to operate at a synchronous phase of -20 deg., and to increase the longitudinal phase spread capture at injection, the first resonator was phased at -40 deg. The last resonator in the first cryomodule was also re-phased, at -30 deg., in

* matteo.pasini@cern.ch

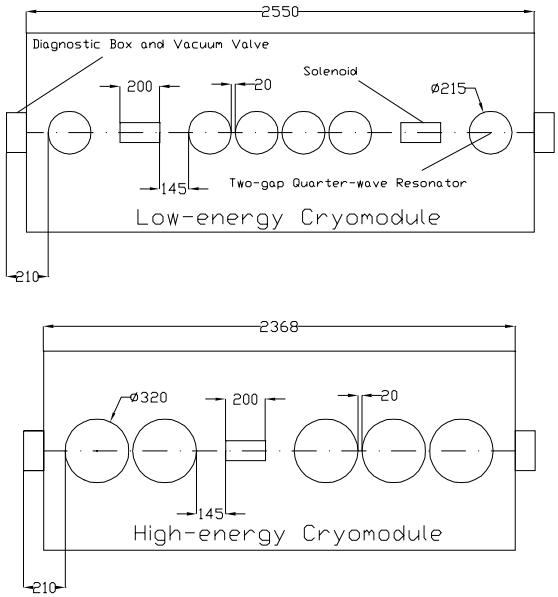

Figure 2: Schematic of the cryomodules design. On the top the low β cryomodule and on the bottom the high β cryomodule.

order to further decrease the longitudinal phase spread of the beam after the first cryomodule. The simulations were implemented to first-order in `LANA` [7] using a square field distribution for the cavities and solenoids and the results confirmed with `Path Manager` [8], which uses a thin-lens approximation for lattice elements. Two thousand particles were simulated and space-charge forces neglected because of the low beam intensity.

The solenoidal magnetic fields were adjusted to achieve matched beams along the HIE-LINAC. The three solenoids in the second and third cryomodules were used to match the beam across the transition region between the low and high-energy sections. Matched solutions were found for different values of the phase advance per cryomodule μ in the low-energy section and the resulting transverse emittance growth along the HIE-LINAC investigated. The source of transverse emittance growth comes essentially from the beam phase spread inside the RF gap, as can be seen from the expression for the RF defocusing impulse, Δp, acting on a single particle, and the growth can be controlled by choosing an appropriate phase advance:

$$\Delta p \propto \frac{\sin(\phi)}{\beta\gamma} r \qquad (1)$$

where r is the particles radial displacement, ϕ is its average longitudinal phase and $\beta\gamma$ are the relativistic factors associated with its motion. From (1), a monotonic decrease in transverse emittance growth would be expected as the phase advance increases and the extent of the beam in the transverse plane shrinks, provided the spread in any of the other variables does not dominate. The results of this preliminary survey are shown in Figure 3, which shows a decrease of emittance growth with phase advance per cryomodule above 80 deg, as expected, but anomalous behaviour below 80 deg.

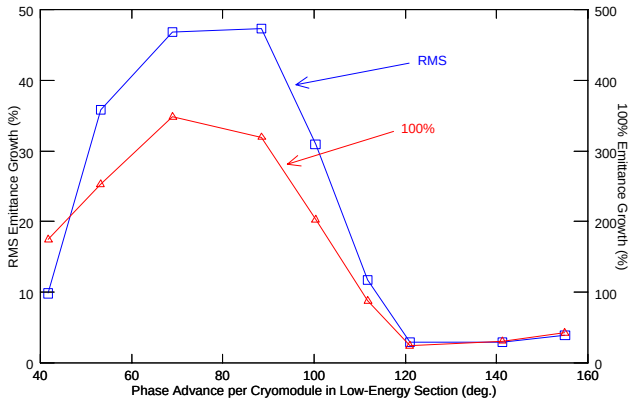

Figure 3: Final emittance growths in the HIE-LINAC with phase advance per cryomodule in the low-energy section.

The variables in Equation 1 are well controlled in the simulations and, in particular, the spread of the longitudinal phase of the beam does not vary enough to account for this anomalous behaviour at low phase advance. This anomalous behaviour was investigated by isolating the low and high-energy sections of the HIE-LINAC and simulating the behaviour of the transverse emittance growth, with phase advance, separately. The input beam parameters for the low-energy section were identical to the previous simulations but the input parameters for the high-energy section were calculated at point B in Figure 1, (i.e. 1664 mm downstream from the 9-gap). The RMS emittance behaves as expected, as shown in Figures 4 and 5, and the transverse emittance growth reduces as the transverse beam size shrinks.

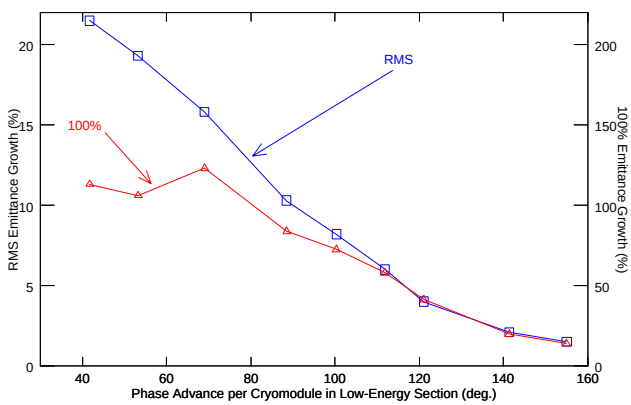

Figure 4: Emittance growth with phase advance in low-energy section.

We conclude that the anomalous behaviour in Figure 3 results from the matching region between the two sections

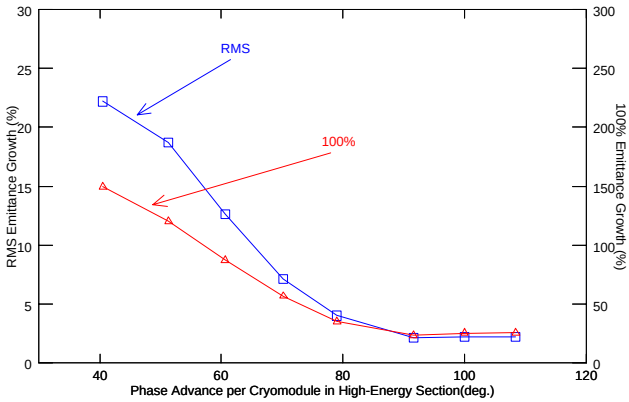

Figure 5: Emittance growth with phase advance in high-energy section.

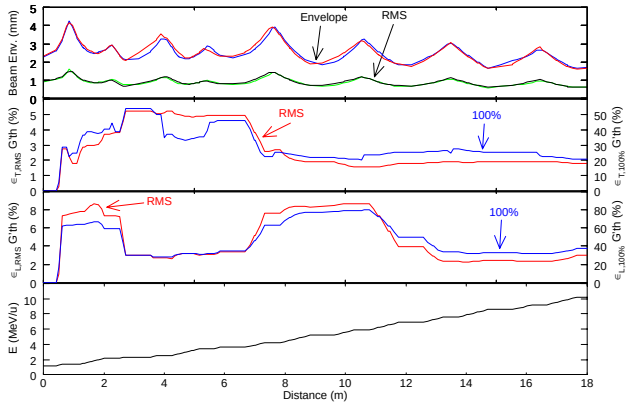

Figure 6: Beam dynamic for a simulation with phase advance of 130 and 90 deg. in the low and high-energy sections, respectively. From top to bottom: max and rms envelope, 100% and rms transverse emittance growth, 100% and rms longitudinal emittance growth, beam energy as a function of the linac length.

of the HIE-LINAC. In order to confine the beam at higher phase advance, larger magnetic fields must be used in the focusing elements. We proceed with the beam dynamics study by selecting the matched solution which provides minimal emittance growth without demanding excessively high solenoidal magnetic fields.

CONCLUSION

Due to the development of the cryomodule design, the inter-cryomodule distance, i.e. the distance from the last cavity in one cryomodule to the first cavity in the following one, was increased to 800 mm; a modification which would have little impact on the findings of our preliminary survey. Both stage 1 and stage 2 scenarios were simulated and the results of the full linac installation are shown in Fig. 6. The chosen matched solution requires 130 deg. phase advance in the first section, and 90 deg. in the second. Both the RMS transverse and longitudinal emittance grow no more than 4% throughout the HIE-LINAC, and, even with the re-phasing of the first and sixth resonators, the target energy of 10 MeV/u is reached, with A/q = 4.5.

The input and output beam parameters are listed in Table 1 for the two installation stages. The average solenoidal magnetic field in the low-energy section is 5.1 T and 7.4 T in the high-energy section.

Future study will aim to better understand the anomalous behaviour observed above. Additional simulations studying the effect of the intrinsic dipole component [9] of the QWRs and higher order effects of the focussing lattice are anticipated. These simulations will focus on field mappings for both the cavity and the solenoids.

Table 1: Beam Parameters

Parameter	Input	Output
Stage 1		
α_T	-0.150	-0.165
β_T (cm/mrad)	0.100	0.132
$\epsilon_{T,100\%,\mathrm{norm}}$ (π cm mrad)	0.030	0.037
α_L	1.425	-0.355
β_L (deg/keV)	0.027	0.038
$\epsilon_{L,100\%,\mathrm{norm}}$ (π ns keV/u)	2.000	2.517
Stage 2		
α_T	-0.200	-0.209
β_T (cm/mrad)	0.100	0.138
$\epsilon_{T,100\%,\mathrm{norm}}$ (π cm mrad)	0.030	0.036
α_L	1.281	1.013
β_L (deg/keV)	0.035	0.044
$\epsilon_{L,100\%,\mathrm{norm}}$ (π ns keV/u)	2.000	2.746

REFERENCES

[1] http://isolde.web.cern.ch/ISOLDE/

[2] M. Lindroos, *et al.*, HIE-ISOLDE : the technical options, CERN-2007-008

[3] M. Pasini, *et al.*, A SC upgrade for the REX-ISOLDE accelerator at CERN, these proc.

[4] R. Laxdal, *et al.*, Progress in the Conceptual Design of the ISAC-II Linac at TRIUMF, PAC2001, Chicago, US

[5] M. Pasini, *et al.*, Beam Dynamics Studies on the ISAC-II Post-Accelerator at TRIUMF, EPAC2002, Paris, France

[6] K.R. Crandall *et al.*, Trace 3-D Documentation, LA-UR-97-886

[7] D. V. Gorelov, P. N. Ostrumov, Application of LANA Code for Design of Ion Linac, Proc. of Linac Conference 1996

[8] A. Perrin and J.F. Amand, Travel v4.06, user manual, CERN (2003).

[9] P. N. Ostroumov and K. W. Shepard, Physical Review STAB, **4**, 110101 (2001)